

Matter-Wave Diffraction from a Quasicrystalline Optical Lattice

Konrad Viebahn, Matteo Sbroscia, Edward Carter, Jr-Chiun Yu, and Ulrich Schneider*
Cavendish Laboratory, University of Cambridge, J. J. Thomson Avenue, Cambridge CB3 0HE, United Kingdom



(Received 26 November 2018; published 20 March 2019)

Quasicrystals are long-range ordered and yet nonperiodic. This interplay results in a wealth of intriguing physical phenomena, such as the inheritance of topological properties from higher dimensions, and the presence of nontrivial structure on all scales. Here, we report on the first experimental demonstration of an eightfold rotationally symmetric optical lattice, realizing a two-dimensional quasicrystalline potential for ultracold atoms. Using matter-wave diffraction we observe the self-similarity of this quasicrystalline structure, in close analogy to the very first discovery of quasicrystals using electron diffraction. The diffraction dynamics on short timescales constitutes a continuous-time quantum walk on a homogeneous four-dimensional tight-binding lattice. These measurements pave the way for quantum simulations in fractal structures and higher dimensions.

DOI: [10.1103/PhysRevLett.122.110404](https://doi.org/10.1103/PhysRevLett.122.110404)

Quasicrystals exhibit long-range order without being periodic [1–6]. Their long-range order manifests itself in sharp diffraction peaks, exactly as in their periodic counterparts. However, diffraction patterns from quasicrystals often reveal rotational symmetries, most notably fivefold, eightfold, and tenfold, that are incompatible with translational symmetry. Therefore, it immediately follows that long-range order in quasicrystals cannot originate from a periodic arrangement of unit cells but requires a different paradigm. Quasicrystalline order naturally arises from an incommensurate projection of a higher-dimensional periodic lattice and thereby enables investigation of physics of higher dimensions, in particular in the context of topology [7–11]. For instance, one-dimensional (1D) quasiperiodic models, such as the Fibonacci chain and the Aubry-Andre model, are closely connected to the celebrated two-dimensional (2D) Harper-Hofstadter model, and inherit their topologically protected edge states [9,11]. An alternative approach to constructing quasicrystals was described by Penrose [12] who discovered a set of tiles and associated matching rules that ensure aperiodic long-range order when tiling a plane [5]. The resulting fivefold symmetric Penrose tiling and the closely related eightfold symmetric octagonal tiling [3,5,13,14] (also known as Ammann-Beenker tiling) have become paradigms of 2D quasicrystals. In addition to their disallowed rotational symmetries, these tilings have the remarkable feature of being self-similar in both real and reciprocal space [2,5]. Self-similarity upon scaling in length by a certain factor (the silver mean $1 + \sqrt{2}$ in the case of the octagonal tiling) implies that nontrivial structure is present on arbitrarily large scales. Correspondingly, diffraction patterns from quasicrystals display sharp peaks at arbitrarily small momenta. Important manifestations of this nontrivial order on all length scales include the absence of universal power-law scaling near criticality [15] and its

application to quantum complexity [16]. Moreover, quasicrystals exhibit fascinating phenomena such as phasonic degrees of freedom [6,17,18]. To date, quasicrystals have been extensively studied in condensed matter and material science [1,3,4,6,17], in photonic structures [9,13,18–20], using laser-cooled atoms in the dissipative regime [21,22], and very recently in twisted bilayer graphene [23]. Quasicrystalline order can even appear spontaneously in dipolar cold-atom systems [24].

In this work, we realize a quasicrystalline potential for ultracold atoms based on an eightfold rotationally symmetric optical lattice, thereby establishing a new experimental platform for the study of quasicrystals. Optical lattices, i.e., standing waves of light, have become a cornerstone in experimental research on quantum many-body physics [25]. They offer an ideal environment for examining quasicrystals since optical potentials are free of defects which greatly complicate measurements on quasicrystalline solids [6]. In addition, we are able to directly impose “forbidden” rotational symmetries, thereby circumventing the elaborate synthesis of stable single crystals [26]. So far, quasiperiodic optical lattices have been used as a proxy for disorder in ultracold quantum gases [27–31], but the intriguing properties of quasicrystalline order have remained unexplored. Here, we use a Bose-Einstein condensate of ^{39}K atoms to probe a quasicrystalline optical lattice in a matter-wave diffraction experiment, namely Kapitza-Dirac scattering [32]. This allows us to observe a self-similar diffraction pattern, similar to those obtained by Shechtman *et al.* using electron diffraction [1] in their original discovery of quasicrystals. Additionally, we investigate the diffraction dynamics which at short times constitutes a continuous-time quantum walk on a four-dimensional (4D) homogeneous tight-binding lattice. Confined synthetic dimensions, which can be created by

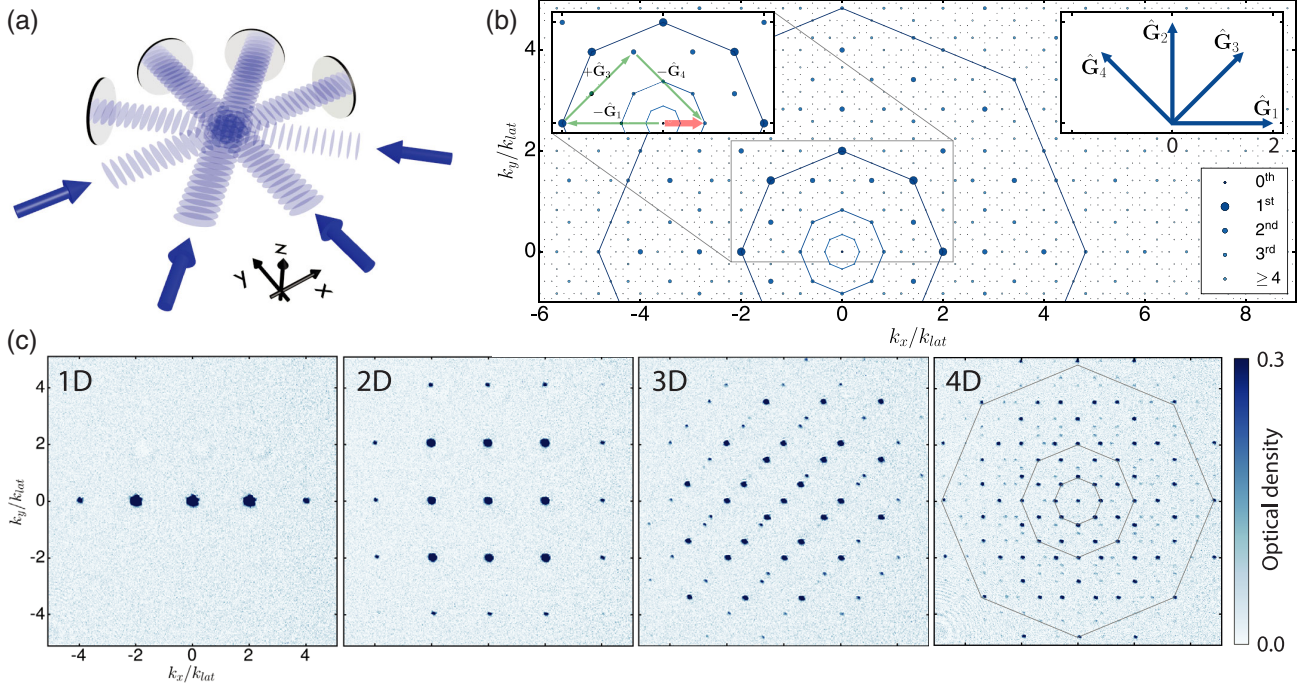


FIG. 1. (a) Schematic of the eightfold optical lattice formed by superimposing four independent 1D lattices. (b) Fractal momentum space structure. The first 15 orders of possible diffraction peaks are shown. They are constructed by iteratively adding or subtracting one of the four reciprocal lattice vectors \hat{G}_i (inset on the right) to the peaks in the previous order, starting with $\mathbf{k} = (0, 0)$. This results in a fractal structure, whose self-similarity is illustrated by a sequence of octagons, which are each scaled by the silver mean $1 + \sqrt{2}$ relative to the next. The left inset shows one inflation step (see text). (c) Raw time-of-flight images resulting from four different lattice configurations at fixed lattice pulse duration ($t = 3.5 \mu\text{s}$). Using just one of the lattice axes results in a regular 1D simple-cubic lattice characterized by \hat{G}_1 ; adding the perpendicular lattice creates a regular 2D square lattice with \hat{G}_1 and \hat{G}_2 . By adding the first diagonal lattice we obtain a regular array of quasiperiodic 1D lattices. These are characterized by a dense set of momentum states along \hat{G}_3 whereas the direction perpendicular to \hat{G}_3 remains periodic (labeled 3D). Finally, using all four axes we create the 2D quasicrystal (labeled 4D) whose self-similarity is illustrated by the octagons.

employing the discrete hyperfine states of atoms, already play an important role in quantum simulation [33–35]. Our measurements demonstrate the potential of quasicrystalline optical lattices to be used for the simulation of extended higher dimensions.

We create the 2D quasicrystalline potential using a planar arrangement of four mutually incoherent 1D optical lattices, each formed by retroreflecting a single-frequency laser beam, as shown schematically in Fig. 1(a). The angle between two neighboring lattice axes is $45(1)^\circ$, similar to the setup proposed in Ref. [14] (see also Refs. [36,37]), thereby imposing a global eightfold rotational symmetry in close analogy to the octagonal tiling. The right inset of Fig. 1(b) shows the reciprocal lattice vectors \hat{G}_1 , \hat{G}_2 , \hat{G}_3 , and \hat{G}_4 of the four 1D lattices. In contrast to a periodic lattice the combination of several \hat{G}_i here may give rise to new, smaller momentum scales, as shown the left inset of Fig. 1(b); for example, the combination $-\hat{G}_1 + \hat{G}_3 - \hat{G}_4$ results in a new k vector (red arrow) that is shorter than the original \hat{G}_1 by a factor of $1 + \sqrt{2}$ (the silver mean). This process can be repeated *ad infinitum* and results in a self-similar fractal structure containing arbitrarily small k

vectors, giving rise to the sequence of octagons in Fig. 1(b). Consequently, it is impossible to assign a maximum characteristic length to this quasicrystal, heralding the presence of structure on all scales. The set of momenta that are reachable from $\mathbf{k}_0 = (0, 0)$ by combining the \hat{G}_i is dense in the k_x, k_y plane and any element \mathbf{G} of this set is determined by four integers $(i, j, l, n) \in \mathbb{Z}^4$ as

$$\mathbf{G} = i\hat{G}_1 + j\hat{G}_2 + l\hat{G}_3 + n\hat{G}_4. \quad (1)$$

While physical momentum remains two dimensional, all four integers are nonetheless required to describe a given \mathbf{G} , since $\cos(45^\circ) = \sin(45^\circ) = 1/\sqrt{2}$ is irrational and hence incommensurable with unity. In fact, Fig. 1(b) can be viewed as an incommensurate projection of a 4D simple-cubic “parent” lattice to the 2D plane, similar to the “cut-and-project” scheme for constructing the octagonal tiling, starting from \mathbb{Z}^4 [5]. By using fewer than four lattice beams we can control the dimensionality of the parent lattice and reduce \mathbb{Z}^4 to \mathbb{Z}^D with $D \in \{1, 2, 3, 4\}$.

The experimental sequence starts with the preparation of an almost pure Bose-Einstein condensate of ^{39}K atoms in a

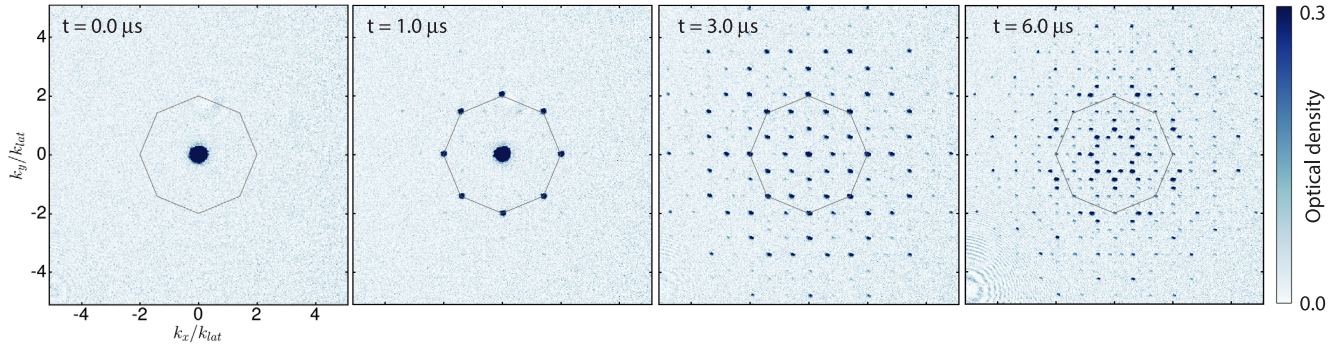


FIG. 2. Dynamics of Kapitza-Dirac diffraction in the quasicrystalline optical lattice. The figure shows raw absorption images for four different lattice pulse durations. After $1 \mu\text{s}$, only the first diffraction order has been populated, while longer pulses lead to populations in successively higher orders as the atoms perform a quantum walk on the fractal momentum structure. Black octagons with a circumradius of $|\hat{\mathbf{G}}_i| = 2k_{\text{lat}}$ illustrate the fundamental momentum scale due to two-photon processes.

crossed-beam dipole trap [38]. Using the Feshbach resonance centered at $402.70(3) \text{ G}$ [45] we tune the contact interaction to zero just before we release the condensate from the trap. Then, we immediately expose it to the optical lattice for a rectangular pulse of duration t . During this pulse, atoms in the condensate can undergo several stimulated two-photon scattering events (Kapitza-Dirac scattering [32]), which scatter photons from one lattice beam into its counterpropagating partner and transfer quantized momenta of $\pm 2\hbar k_{\text{lat}}$, where $\hbar k_{\text{lat}}$ is the momentum of a lattice photon and $|\hat{\mathbf{G}}_i| = 2k_{\text{lat}}$. The lattice wavelength $\lambda_{\text{lat}} = 2\pi/k_{\text{lat}} = 726 \text{ nm}$ is far detuned from the D lines in ^{39}K , ensuring that single-photon processes are completely suppressed. Throughout this work, the lattice depth of each individual axis is $14.6(2)E_{\text{rec}}$, with $E_{\text{rec}} = \hbar^2/(2m\lambda_{\text{lat}}^2)$ denoting the recoil energy, m being the atomic mass and \hbar being Planck's constant. Finally, we record the momentum distribution of the atomic cloud by taking an absorption image after 33 ms time of flight [38].

In a first experiment we fix the lattice pulse duration at $t = 3.5 \mu\text{s}$ and vary the number of lattice beams, as shown in Fig. 1(c). Starting from the single-axis (1D) case, we subsequently add lattice axes, finally completing the eightfold symmetric case (4D), representing the quasicrystalline structure with its striking self-similarity under $(1 + \sqrt{2})$ scaling.

The diffraction dynamics offers additional signatures of the fractal nature of the eightfold optical lattice: during the lattice pulse the condensate explores reciprocal space in discrete steps of $\pm \hat{\mathbf{G}}_i$, leading to profoundly distinct behaviors in the periodic (2D) and in the quasicrystalline case (4D). Figure 2 shows absorption images for four different values of pulse duration t in the latter configuration, illustrating the occupation of more and more closely spaced momenta. Using individual fits [38] we extract the number of atoms in every k state up to the seventh diffraction order, i.e., those momenta reachable by seven or fewer two-photon scattering events. In all cases, high

momentum states are inaccessible, as the corresponding two-photon transitions become off-resonant due to kinetic energy. Therefore, in the 2D simple-cubic lattice (Fig. 3 on the left) the total number of accessible states is limited and the dynamics is oscillatory, reminiscent of a simple harmonic oscillator. In the quasicrystalline case (4D, right of Fig. 3), in contrast, the diffraction dynamics is non-oscillatory: due to the fractal momentum space structure,

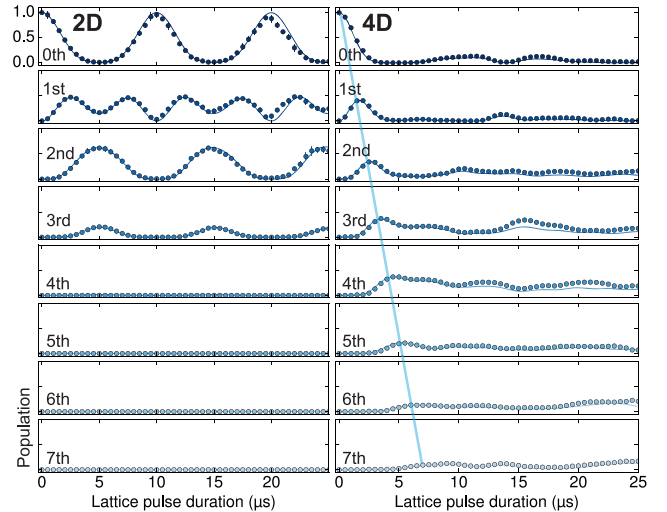


FIG. 3. Kapitza-Dirac diffraction dynamics in a periodic (2D) and quasicrystalline (4D) lattice. The normalized populations (colored dots) of the condensate (0th order) and the first seven diffraction orders are plotted against pulse duration, together with the numerical solution to the Schrödinger equation (lines). The periodic case (2D) is oscillatory as kinetic energy limits the accessible momenta. In contrast, the quasicrystalline lattice (4D) contains a fractal set of k states, cf. Fig. 1(b), enabling the population of higher and higher orders without kinetic energy penalty. Correspondingly, the expansion carries on linearly, indicated by the light blue “wave front” as a guide to the eye. Error bars denote the standard deviations from five realizations of the experiment, and are typically smaller than symbol size.

the atoms can access states in ever higher diffraction orders that correspond to ever smaller momenta. As a consequence, large parts of the population propagate ballistically to progressively higher orders, as illustrated by the light blue “light cone.” Our data agree excellently with exact numerical solutions (lines in Fig. 3) of the single-particle time-dependent Schrödinger equation in momentum basis [38].

In the regime of short pulses, the Fourier limit ensures that kinetic energy can be neglected for all dimensions and the discrete momentum space structure can be seen as a homogeneous tight-binding lattice [46,47]. A hopping event in this effective lattice corresponds to a two-photon scattering event and connects momenta differing by $\pm\hbar\hat{G}_i$. In this picture, the diffraction dynamics is equivalent to the expansion of initially localized particles in this synthetic lattice and gives rise to a continuous-time quantum walk with its characteristic light-cone-like propagation [48–50]. For a hypercubic lattice in D dimensions, the separability of the tight-binding dispersion relation leads to an average group velocity proportional to \sqrt{D} [38]. Because of the correspondence between the number of lattice beams and the dimension of the resulting tight-binding Hamiltonian, we are able to extend the dynamics to up to four dimensions. Using the appropriate form of Eq. (1) in \mathbb{Z}^D , we extract the effective root-mean-square momentum

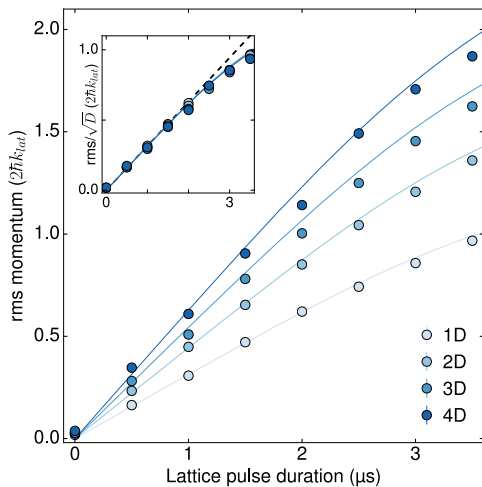


FIG. 4. Continuous-time quantum walk in D dimensions, where D is controlled by the number of lattice beams. Dots represent the measured root-mean-square momentum (see text), while lines represent numerical solutions to the full Schrödinger equation. The inset shows the same data, but scaled by \sqrt{D} . Here, the dashed line represents the expansion dynamics of a continuous-time quantum walk on a homogeneous D -dimensional tight-binding lattice. The \sqrt{D} scaling (Eq. S13 in the Supplemental Material [38]) is a direct consequence of the separability of hypercubic lattices. Deviations from the linear behavior at later times are due to kinetic energy, and the lines would differ from each other at long times [38]. Error bars denote standard deviations from five identical realizations of the experiment.

in D dimensions, e.g., $\sqrt{\langle i^2 + j^2 \rangle}$ in the 2D case and $\sqrt{\langle i^2 + j^2 + l^2 + n^2 \rangle}$ in the 4D case, from the individual populations of all diffraction peaks, and find excellent agreement between the measurements and the analytic result $v_p \propto \sqrt{D}$ [38], as shown in Fig. 4. The departure from linear behavior at longer times is due to kinetic energy and is captured well by the exact numerical solution to the Schrödinger equation (solid lines in Fig. 4). The extent of the linear region is controlled by the lattice depth. For even longer times, kinetic energy enforces fundamentally different behaviors for periodic and quasicrystalline lattices, as shown in Fig. 3 (and in Fig. S3 in the Supplemental Material [38]).

In conclusion, we have realized a quasicrystalline potential for ultracold atoms, which can facilitate the creation of ever more complex many-body systems [16] and novel phases [51]. By observing the occupation of successively closer-spaced momenta, we were able to confirm its self-similar fractal structure in momentum space. In addition, we experimentally verified the fundamentally different diffraction dynamics between periodic and quasicrystalline potentials, in excellent agreement with theory. Finally, we demonstrated the ability to simulate tight-binding models in one to four dimensions, by observing the light-cone-like spreading of particles in reciprocal space. On the one hand, these measurements pave the way for more elaborate quantum simulations in four dimensions, including topological effects and charge pumps [10,52]. On the other hand, quasicrystalline potentials enable experimental studies of novel quantum phenomena that have been predicted for quasicrystals, such as non-power-law criticality [15], topological edge states [7,11,53], and spiral holonomies [54]. Finally, our system will provide unprecedented access to transport and localization properties of quasicrystals, thereby addressing fundamental questions about the relation between quasiperiodic order and randomness [55] and extending studies of many-body localization and Bose glasses to two dimensions [29,30,56,57].

We would like to thank Oliver Brix, Michael Höse, Max Melchner, and Hendrik von Raven for assistance during the construction of the experiment. We are grateful to Dmytro Bondarenko and Anuradha Jagannathan, as well as Zoran Hadzibabic, Rob Smith, and their team for helpful discussions. This work was partly funded by the European Commission ERC starting Grant No. QUASICRYSTAL and the EPSRC Programme Grant No. DesOEq (EP/P009565/1).

*uws20@cam.ac.uk

[1] D. Shechtman, I. Blech, D. Gratias, and J. W. Cahn, Metallic Phase with Long-Range Orientational Order and No Translational Symmetry, *Phys. Rev. Lett.* **53**, 1951 (1984).

- [2] M. Senechal, *Quasicrystals and Geometry* (Cambridge University Press, Cambridge, England, 1995).
- [3] W. Steurer, Twenty years of structure research on quasicrystals. Part I. Pentagonal, octagonal, decagonal and dodecagonal quasicrystals, *Z. Kristallogr. Cryst. Mater.* **219**, 391 (2004).
- [4] E. Maciá Barber, *Aperiodic Structures in Condensed Matter: Fundamentals and Applications*, Condensed Matter Physics (CRC Press, Boca Raton, London, 2009).
- [5] *A Mathematical Invitation*, edited by M. Baake and U. Grimm, Aperiodic Order Vol. 1 (Cambridge University Press, Cambridge, England, 2013).
- [6] W. Steurer, Quasicrystals: What do we know? What do we want to know? What can we know? *Acta Crystallogr. Sect. A* **74**, 1 (2018).
- [7] L.-J. Lang, X. Cai, and S. Chen, Edge States and Topological Phases in One-Dimensional Optical Superlattices, *Phys. Rev. Lett.* **108**, 220401 (2012).
- [8] Y. E. Kraus, Y. Lahini, Z. Ringel, M. Verbin, and O. Zeitler, Topological States and Adiabatic Pumping in Quasicrystals, *Phys. Rev. Lett.* **109**, 106402 (2012).
- [9] Y. E. Kraus and O. Zeitler, Topological Equivalence between the Fibonacci Quasicrystal and the Harper Model, *Phys. Rev. Lett.* **109**, 116404 (2012).
- [10] Y. E. Kraus, Z. Ringel, and O. Zeitler, Four-Dimensional Quantum Hall Effect in a Two-Dimensional Quasicrystal, *Phys. Rev. Lett.* **111**, 226401 (2013).
- [11] F. Matsuda, M. Tezuka, and N. Kawakami, Topological Properties of Ultracold Bosons in One-Dimensional Quasiperiodic Optical Lattice, *J. Phys. Soc. Jpn.* **83**, 083707 (2014).
- [12] R. Penrose, The Rôle of Aesthetics in Pure and Applied Mathematical Research, *Bull. Inst. Math. Appl.* **10**, 266 (1974).
- [13] Y. S. Chan, C. T. Chan, and Z. Y. Liu, Photonic Band Gaps in Two Dimensional Photonic Quasicrystals, *Phys. Rev. Lett.* **80**, 956 (1998).
- [14] A. Jagannathan and M. Duneau, An eightfold optical quasicrystal with cold atoms, *Europhys. Lett.* **104**, 66003 (2013).
- [15] A. Szabó and U. Schneider, Non-power-law universality in one-dimensional quasicrystals, *Phys. Rev. B* **98**, 134201 (2018).
- [16] T. S. Cubitt, D. Perez-Garcia, and M. M. Wolf, Undecidability of the spectral gap, *Nature (London)* **528**, 207 (2015).
- [17] K. Edagawa, K. Suzuki, and S. Takeuchi, High Resolution Transmission Electron Microscopy Observation of Thermally Fluctuating Phasons in Decagonal Al-Cu-Co, *Phys. Rev. Lett.* **85**, 1674 (2000).
- [18] B. Freedman, G. Bartal, M. Segev, R. Lifshitz, D. N. Christodoulides, and J. W. Fleischer, Wave and defect dynamics in nonlinear photonic quasicrystals, *Nature (London)* **440**, 1166 (2006).
- [19] J. Mikhael, J. Roth, L. Helden, and C. Bechinger, Archimedean-like tiling on decagonal quasicrystalline surfaces, *Nature (London)* **454**, 501 (2008).
- [20] A. Dureau, E. Levy, M. B. Aguilera, R. Bouganne, E. Akkermans, F. Gerbier, and J. Beugnon, Revealing the Topology of Quasicrystals with a Diffraction Experiment, *Phys. Rev. Lett.* **119**, 215304 (2017).
- [21] L. Guidoni, C. Triché, P. Verkerk, and G. Grynberg, Quasiperiodic Optical Lattices, *Phys. Rev. Lett.* **79**, 3363 (1997).
- [22] L. Guidoni, B. Dépret, A. di Stefano, and P. Verkerk, Atomic diffusion in an optical quasicrystal with five-fold symmetry, *Phys. Rev. A* **60**, R4233 (1999).
- [23] S. J. Ahn, P. Moon, T.-H. Kim, H.-W. Kim, H.-C. Shin, E. H. Kim, H. W. Cha, S.-J. Kahng, P. Kim, M. Koshino, Y.-W. Son, C.-W. Yang, and J. R. Ahn, Dirac electrons in a dodecagonal graphene quasicrystal, *Science* **361**, 782 (2018).
- [24] S. Gopalakrishnan, I. Martin, and E. A. Demler, Quantum Quasicrystals of Spin-Orbit-Coupled Dipolar Bosons, *Phys. Rev. Lett.* **111**, 185304 (2013).
- [25] I. Bloch, J. Dalibard, and S. Nascimbène, Quantum simulations with ultracold quantum gases, *Nat. Phys.* **8**, 267 (2012).
- [26] M. Feuerbacher, C. Thomas, K. Urban, R. Lück, L. Zhang, R. Sterzel, E. Uhrig, E. Dahlmann, A. Langsdorf, W. Assmus, U. Köster, D. Zander, L. Lyubenova, L. Jastrow, P. Gille, R.-U. Barz, and L. M. Zhang, *Synthesis, Metallurgy and Characterization, Quasicrystals* (John Wiley & Sons, New York, 2006), pp. 1–87.
- [27] J. E. Lye, L. Fallani, C. Fort, V. Guarrera, M. Modugno, D. S. Wiersma, and M. Inguscio, Effect of interactions on the localization of a Bose-Einstein condensate in a quasiperiodic lattice, *Phys. Rev. A* **75**, 061603 (2007).
- [28] G. Roati, C. D’Errico, L. Fallani, M. Fattori, C. Fort, M. Zaccanti, G. Modugno, M. Modugno, and M. Inguscio, Anderson localization of a non-interacting Bose-Einstein condensate, *Nature (London)* **453**, 895 (2008).
- [29] C. D’Errico, E. Lucioni, L. Tanzi, L. Gori, G. Roux, I. P. McCulloch, T. Giamarchi, M. Inguscio, and G. Modugno, Observation of a Disordered Bosonic Insulator from Weak to Strong Interactions, *Phys. Rev. Lett.* **113**, 095301 (2014).
- [30] M. Schreiber, S. S. Hodgman, P. Bordia, H. P. Lüschen, M. H. Fischer, R. Vosk, E. Altman, U. Schneider, and I. Bloch, Observation of many-body localization of interacting fermions in a quasirandom optical lattice, *Science* **349**, 842 (2015).
- [31] P. Bordia, H. Lüschen, S. Scherg, S. Gopalakrishnan, M. Knap, U. Schneider, and I. Bloch, Probing Slow Relaxation and Many-Body Localization in Two-Dimensional Quasiperiodic Systems, *Phys. Rev. X* **7**, 041047 (2017).
- [32] S. Gupta, A. E. Leanhardt, A. D. Cronin, and D. E. Pritchard, Coherent manipulation of atoms with standing light waves, *C. R. Acad. Sci. Paris* **2**, 479 (2001).
- [33] A. Celi, P. Massignan, J. Ruseckas, N. Goldman, I. B. Spielman, G. Juzeliūnas, and M. Lewenstein, Synthetic Gauge Fields in Synthetic Dimensions, *Phys. Rev. Lett.* **112**, 043001 (2014).
- [34] M. Mancini, G. Pagano, G. Cappellini, L. Livi, M. Rider, J. Catani, C. Sias, P. Zoller, M. Inguscio, M. Dalmonte, and L. Fallani, Observation of chiral edge states with neutral fermions in synthetic Hall ribbons, *Science* **349**, 1510 (2015).
- [35] H. M. Price, O. Zeitler, T. Ozawa, I. Carusotto, and N. Goldman, Four-Dimensional Quantum Hall Effect with Ultracold Atoms, *Phys. Rev. Lett.* **115**, 195303 (2015).
- [36] L. Sanchez-Palencia and L. Santos, Bose-Einstein condensates in optical quasicrystal lattices, *Phys. Rev. A* **72**, 053607 (2005).

- [37] A. Cetoli and E. Lundh, Loss of coherence and superfluid depletion in an optical quasicrystal, *J. Phys. B* **46**, 085302 (2013).
- [38] See Supplemental Material at <http://link.aps.org/supplemental/10.1103/PhysRevLett.122.110404>, which includes Refs. [39–44], for further experimental details, theoretical calculations, and data analysis.
- [39] K. Dieckmann, R. J. C. Spreeuw, M. Weidemüller, and J. T. M. Walraven, Two-dimensional magneto-optical trap as a source of slow atoms, *Phys. Rev. A* **58**, 3891 (1998).
- [40] W. Ketterle, K. B. Davis, M. A. Joffe, A. Martin, and D. E. Pritchard, High Densities of Cold Atoms in a Dark Spontaneous-Force Optical Trap, *Phys. Rev. Lett.* **70**, 2253 (1993).
- [41] M. Greiner, I. Bloch, T. W. Hänsch, and T. Esslinger, Magnetic transport of trapped cold atoms over a large distance, *Phys. Rev. A* **63**, 031401 (2001).
- [42] A. Simoni, M. Zaccanti, C. D’Errico, M. Fattori, G. Roati, M. Inguscio, and G. Modugno, Near-threshold model for ultracold KRb dimers from interisotope Feshbach spectroscopy, *Phys. Rev. A* **77**, 052705 (2008).
- [43] A. P. Chikkatur, A. Görlitz, D. M. Stamper-Kurn, S. Inouye, S. Gupta, and W. Ketterle, Suppression and Enhancement of Impurity Scattering in a Bose-Einstein Condensate, *Phys. Rev. Lett.* **85**, 483 (2000).
- [44] M. Greiner, I. Bloch, O. Mandel, T. Hänsch, and T. Esslinger, Exploring Phase Coherence in a 2D Lattice of Bose-Einstein Condensates, *Phys. Rev. Lett.* **87**, 160405 (2001).
- [45] R. J. Fletcher, R. Lopes, J. Man, N. Navon, R. P. Smith, M. W. Zwierlein, and Z. Hadzibabic, Two- and three-body contacts in the unitary Bose gas, *Science* **355**, 377 (2017).
- [46] B. Gadway, Atom-optics approach to studying transport phenomena, *Phys. Rev. A* **92**, 043606 (2015).
- [47] S. Dadras, A. Gresch, C. Groiseau, S. Wimberger, and G. S. Summy, Quantum Walk in Momentum Space with a Bose-Einstein Condensate, *Phys. Rev. Lett.* **121**, 070402 (2018).
- [48] C. Weitenberg, M. Endres, J. F. Sherson, M. Cheneau, P. Schauß, T. Fukuhara, I. Bloch, and S. Kuhr, Single-spin addressing in an atomic Mott insulator, *Nature (London)* **471**, 319 (2011).
- [49] U. Schneider, L. Hackermüller, J. P. Ronzheimer, S. Will, S. Braun, T. Best, I. Bloch, E. Demler, S. Mandt, D. Rasch, and A. Rosch, Fermionic transport and out-of-equilibrium dynamics in a homogeneous Hubbard model with ultracold atoms, *Nat. Phys.* **8**, 213 (2012).
- [50] P. M. Preiss, M. Ruichao, M. Eric Tai, A. Lukin, M. Rispoli, P. Zupancic, Y. Lahini, R. Islam, and M. Greiner, Strongly correlated quantum walks in optical lattices, *Science* **347**, 1229 (2015).
- [51] A. M. Rey, I. I. Satija, and C. W. Clark, Quantum coherence of hard-core bosons: Extended, glassy, and Mott phases, *Phys. Rev. A* **73**, 063610 (2006).
- [52] M. Lohse, C. Schweizer, H. M. Price, O. Zilberberg, and I. Bloch, Exploring 4D quantum Hall physics with a 2D topological charge pump, *Nature (London)* **553**, 55 (2018).
- [53] K. Singh, K. Saha, S. A. Parameswaran, and D. M. Weld, Fibonacci optical lattices for tunable quantum quasicrystals, *Phys. Rev. A* **92**, 063426 (2015).
- [54] S. Spurrier and N. R. Cooper, Semiclassical dynamics, Berry curvature, and spiral holonomy in optical quasicrystals, *Phys. Rev. A* **97**, 043603 (2018).
- [55] V. Khemani, D. N. Sheng, and D. A. Huse, Two Universality Classes for the Many-Body Localization Transition, *Phys. Rev. Lett.* **119**, 075702 (2017).
- [56] C. Meldgin, U. Ray, P. Russ, D. Chen, D. M. Ceperley, and B. DeMarco, Probing the Bose glass–superfluid transition using quantum quenches of disorder, *Nat. Phys.* **12**, 646 (2016).
- [57] Ş. G. Söyler, M. Kiselev, N. V. Prokof’ev, and B. V. Svistunov, Phase Diagram of the Commensurate Two-Dimensional Disordered Bose-Hubbard Model, *Phys. Rev. Lett.* **107**, 185301 (2011).